A Decentralized Adaptive SOC Balancing Strategy in VSG-based Islanded Power System

Chen, Meng; Zhou, Dao; Blaabjerg, Frede

Published in:
IECON 2021 – 47th Annual Conference of the IEEE Industrial Electronics Society

DOI (link to publication from Publisher):
10.1109/IECON48115.2021.9589320

Publication date:
2021

Document Version
Accepted author manuscript, peer reviewed version

A Decentralized Adaptive SOC Balancing Strategy in VSG-based Islanded Power System

Meng Chen, Dao Zhou, and Frede Blaabjerg
AAU Energy
Aalborg University
Aalborg, Denmark
mche@energy.aau.dk, zda@energy.aau.dk, fbl@energy.aau.dk

***Abstract*—The unbalance of the state-of-charges (SOCs) may be among paralleled energy storage systems (ESSs) is harmful for the system operation. This paper proposes an adaptive control strategy to achieve the balance of SOCs among the paralleled ESS-based virtual synchronous generators (VSGs) in a completely decentralized way. The parameters of the virtual governor are designed to change according to the local SOC taking the stability and steady-state frequency limitation into consideration. To realize the adaptive control, this paper starts with an analysis of the generalized requirements of the adaptive terms. Then linear relationships are chosen as an example to construct the adaptive controller. The IEEE 9-Bus system is used to verify that, with the proposed method, the SOC balancing can be gradually realized no matter the differences in the initial values and disturbances without the communication network.**

***Index Terms*—state-of-charge, adaptive control, virtual synchronous generator, droop control, energy storage system**

I. Introduction

To solve the challenges introduced by the inverter-interfaced generators using a common grid-following control strategy, the virtual synchronous generator (VSG), which usually behaves as a grid-forming inverter, is proposed to emulate the synchronous generator (SG) characteristics [1]. To realize an VSG, an energy reserve is necessary in order to provide both the short-term inertia support and the long-term frequency regulation, where the energy storage system (ESS) is a promising choice due to its high energy density and flexible bidirectional flow of power [2]. The VSG controlled ESS can be used to provide many services for the power system, such as inertia provision, frequency and voltage regulation, etc. [3], [4].

From the perspective of reliability, it is preferable that the state-of-charges (SOCs) are equal when more than one ESS are connected into a power system. Otherwise, some ESSs with lower SOCs may be out of operation leading to abnormal situations of the power system, while other ESSs actually still have much reserved energy [5]. However, it is hard to guarantee the initial SOC to be exactly identical with others when a new ESS is connected. Even though all the SOCs of the ESSs can be set as the same at a certain instant, they may deviate from each other due to unbalanced transient and steady-state power sharing if there is no additional SOC balancing control mechanism [6].

In general, the SOC balancing can be achieved with or without the communication networks [7]–[14]. When a communication network is available, the SOC is usually regulated at the secondary control level, where both the local and some global information can be obtained. In [7], a centralized secondary controller is used to adjust the droop coefficient of ESSs according to their SOCs, while, in [8] and [9], the distributed secondary control structure is designed, which uses the netted communication network to change the set-point values and then decrease the SOC differences among ESSs. On the contrary, in the case of no communication network, only the local information can be obtained to construct a completely decentralized control structure. In [10] and [11], the droop coefficient is related to the local SOC, where the output power of the ESS to a DC grid, therefore, is changed automatically according to the remaining energy. A similar idea is applied to an AC grid in [12], where the regulation speed of this method is related to the maximum range of the droop coefficient variation. However, the droop coefficient may highly influence the stability of the system, which is not supposed to change much. In [13], this problem may be solved by adding an SOC droop control. However, it does not consider the steady-state frequency limitations. Another decentralized SOC balancing control is proposed in [14] based on the filter-based design, where only a DC grid is studied.

This paper aims to achieve the SOC balancing for a VSG-based AC islanded power system using a decentralized strategy. In order to take care of both the stability and frequency limitation, the droop coefficient and the set-point value of the virtual governor are adaptively regulated based on the local SOC. The general requirement of the adaptive terms are discussed, and from this point, the aforementioned decentralized methods are special cases with specific adaptive terms. Afterwards, the linear relationships are chosen to propose a new SOC-balancing controller.

The rest of this paper is organized as follows. The basic principle of VSG is given in Section II. In Section III, the proposed adaptive SOC balancing control is presented in details. Section IV shows the simulation results. Finally, the conclusions are drawn in Section V.

II. Basic principle of Virtual Synchronous Generator

The topology of the VSG with the proposed control strategy is shown in Fig. 1, where the virtual rotor and the virtual wind-

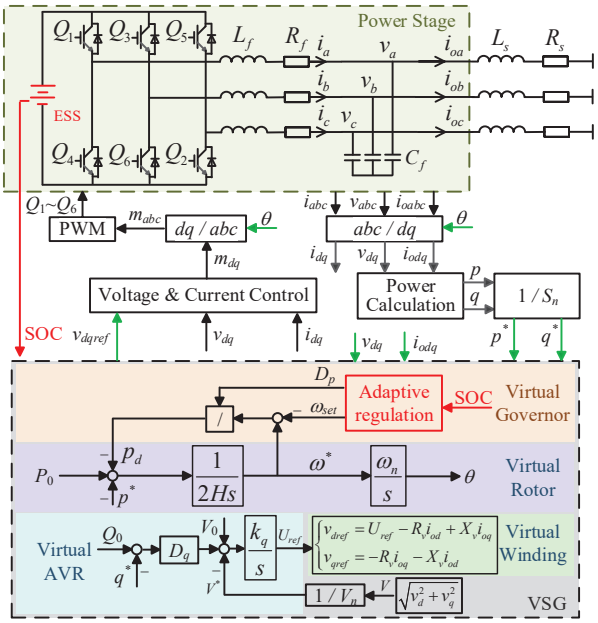

Fig. 1. Block diagram of VSG with the proposed SOC balancing control

ing emulate the inertial and electromagnetic characteristics of a synchronous generator (SG), the virtual governor and the virtual automatic voltage regulator (AVR) emulate the control system of an SG. The control system is built in the d-q frame using p.u. values.

Based on Fig. 1, the relationship between the frequency and active power of the VSG is dominated by

$$\begin{cases} 2H\dfrac{d\omega^*}{dt} = P_0 - p^* - \dfrac{1}{D_p}(\omega^* - \omega_{set}) \\ \dfrac{d\theta}{dt} = \omega_n \omega^* \end{cases} \tag{1}$$

where P_0 and p^* are the set-point and actual values of the output active power, ω_{set} and ω^* are the set-point and actual values of the angle frequency, D_p is the droop coefficient, and H is the inertia constant. θ is the rotor angle to define the d-q frame. Unlike the traditional VSG control with constant parameters, both ω_{set} and D_p of the proposed SOC balancing control strategy are adaptively changeable based on the SOC of the ESS and the specification of the system, which will be discussed in Section III.

Moreover, the relationship between the voltage and reactive power of the VSG is dominated by

$$U_{ref} = k_q \int [V_0 - V^* + D_q(Q_0 - q^*)]dt \tag{2}$$

where Q_0 and q^* are the set-point and actual values of the output reactive power, V_0 and V^* are the set-point and actual values of the terminal voltage, D_q is the droop coefficient of the virtual AVR. In addition, U_{ref} is the derived internal voltage of the VSG, which is further used as the input of the virtual winding as shown in Fig. 1. The mathematical model of the virtual winding is expressed as

$$v_{dref} = U_{ref} - R_v i_{od} + X_v i_{oq} \tag{3}$$

$$v_{qref} = -R_v i_{oq} - X_v i_{od} \tag{4}$$

where R_v and X_v are the virtual resistance and virtual synchronous reactance, i_{od} and i_{oq} are the output currents. Thereafter, the inner voltage and current loops are used to regulate the capacitor voltage and inductor current of the filter.

In order to well behave the short-term inertial characteristics and the long-term frequency regulation, the DC source of the VSG should have enough energy reserve, where the ESS is one of the promising choices.

III. Adaptive State-of-Charge Balancing Control

To achieve the SOC balancing of the ESSs among different VSGs, the parameters of the virtual governor are designed as adaptive terms, which are functions of the local SOC and can be expressed as

$$\begin{cases} D_p = f(SOC) > 0 \\ \omega_{set} = g(SOC) > 0 \end{cases} \tag{5}$$

where $f(SOC)$ and $g(SOC)$ are functions of SOC, which are going to be discussed and designed in the following. The real-time SOC can be obtained from the battery management system or estimated using the traditional Coulomb method as given in [15]

$$SOC = SOC_{ini} - \frac{1}{E_{ESS}V_{dc}} \int pdt \tag{6}$$

where SOC_{ini} is the initial SOC, E_{ESS} is the capacity of the ESS, and V_{dc} is the DC voltage.

A. General Requirements of Adaptive Terms

To deal with both charge and discharge stage, P_0 is set to zero. Meanwhile, the change of SOC is much slower compared with the function of inertia. Therefore, according to (1), the output active power can be calculated as

$$p^* = -\frac{1}{f(SOC)}\omega^* + \frac{g(SOC)}{f(SOC)} \tag{7}$$

Firstly, $g(SOC)$ is designed to be a monotonically non-decreasing function of SOC as

$$\frac{dg(SOC)}{dSOC} \geq 0 \tag{8}$$

which is because it is easier to set a higher frequency with more energy reserve. Suppose ESSi and ESSj are two VSG-based units connected in the system, and assume the relationship of the SOC at $t = t_0$ is $SOC_i > SOC_j$. Therefore, $g(SOC_i) \geq g(SOC_j)$.

Then, there should be $p_i^* \geq p_j^*$ in order to decrease the difference between SOC_i and SOC_j. Considering (7), the following inequality should be guaranteed

$$-\frac{1}{f(SOC_i)}\omega^* + \frac{g(SOC_i)}{f(SOC_i)} \geq -\frac{1}{f(SOC_j)}\omega^* + \frac{g(SOC_j)}{f(SOC_j)} \tag{9}$$

which will be used to determine the features of $f(SOC)$.

With respect to ω^*, there are three possible cases as given in the following

Case 1 $\omega^* < g(SOC_j)$: Based on (7), this case is also represented by the active power as

$$\omega^* < g(SOC_j) \Leftrightarrow p_i^* > 0,\ p_j^* > 0 \tag{10}$$

Furthermore, according to the monotonicity of $g(SOC)$, there is

$$-\frac{1}{f(SOC_i)}\omega^* + \frac{g(SOC_i)}{f(SOC_i)} \geq -\frac{1}{f(SOC_i)}\omega^* + \frac{g(SOC_j)}{f(SOC_i)} \tag{11}$$

By comparing (9) and (11), it is concluded that (9) can be sufficiently guaranteed if the following inequality holds

$$-\frac{1}{f(SOC_i)}\omega^* + \frac{g(SOC_j)}{f(SOC_i)} \geq -\frac{1}{f(SOC_j)}\omega^* + \frac{g(SOC_j)}{f(SOC_j)} \tag{12}$$

which can be rewritten as

$$[\frac{1}{f(SOC_j)} - \frac{1}{f(SOC_i)}][\omega^* - g(SOC_j)] \geq 0 \tag{13}$$

Therefore, in this case, there is

$$f(SOC_i) \leq f(SOC_j) \Rightarrow p_i^* \geq p_j^* \tag{14}$$

Case 2 $g(SOC_j) \leq \omega^* < g(SOC_i)$: Similarly, this case is also represented by the active power as

$$g(SOC_j) \leq \omega^* < g(SOC_i) \Leftrightarrow p_i^* > 0,\ p_j^* \leq 0 \tag{15}$$

which implies that there always is $p_i^* \geq p_j^*$.

Case 3 $\omega^* \geq g(SOC_i)$: This case is also represented by the active power as

$$\omega^* \geq g(SOC_i) \Leftrightarrow p_i^* \leq 0,\ p_j^* \leq 0 \tag{16}$$

According to (13), in this case, there is

$$f(SOC_i) \geq f(SOC_j) \Rightarrow p_i^* \geq p_j^* \tag{17}$$

By combining the conclusions of the aforementioned three cases as well as in (8), a sufficient condition of the adaptive terms is expressed as

$$\frac{dg(SOC)}{dSOC} \geq 0 \ \cap\ \frac{df(SOC)}{dSOC} \begin{cases} \leq 0,\ p^* \geq 0 \\ > 0,\ p^* < 0 \end{cases} \tag{18}$$

which, as shown, also takes the charge/discharge states into consideration. It should be mentioned that, in order to well decrease the distinctions of the SOCs, the equal signs should not work simultaneously.

Table I summarizes some existing decentralized SOC balancing control strategies in the literature. As shown, all of them satisfy (18), which can be concluded that (18) gives a general requirement of the adaptive terms. A proposed method is also included in Table I for comparison, which will be illustrated in the following.

B. Adaptive terms design based on linear relationships

There are infinite choices satisfying (18). Among them, the linear relationships between the SOC and the adaptive terms are ones of the simplest, which are used in this paper. Unlike the existing methods such as given in Table I, both the $g(SOC)$ and $f(SOC)$ are designed in this paper.

As the linear relationships are used, according to (18), $g(SOC)$ and $f(SOC)$ are designed as following

$$\begin{aligned} g(SOC) &= a_g SOC + b_g \\ f(SOC) &= \begin{cases} -a_{f1}SOC + b_{f1},\ p^* \geq 0 \\ a_{f2}SOC + b_{f2},\ p^* < 0 \end{cases} \end{aligned} \tag{19}$$

where $a_g > 0$, $a_{f1} > 0$, $a_{f2} > 0$, b_g, b_{f1}, and b_{f2} are parameters to be determined. In this paper, the following specifications are considered.

1) SOC limitation: The SOC in normal operation is assumed to be between 30% and 100%.
2) Stability limitation: $f(SOC)$ can vary between 0.004 p.u. and 0.01 p.u. from the perspectives of both stability and power sharing.
3) Output power limitation: The output power p^* is assumed to be between -1 and 1 p.u. in the steady-state.
4) Frequency limitation: The frequency is assumed to be between 0.99 and 1.02 p.u. in the steady-state..

Firstly, according to 1) and 2), the parameters of $f(SOC)$ can be derived by

$$\begin{cases} -0.3a_{f1} + b_{f1} = 0.01 \\ -a_{f1} + b_{f1} = 0.004 \\ a_{f2} + b_{f2} = 0.01 \\ 0.3a_{f2} + b_{f2} = 0.004 \end{cases} \tag{20}$$

which yields $a_{f1} = 3/350$, $b_{f1} = 4.4/350$, $a_{f2} = 3/350$, and $b_{f2} = 0.5/350$.

Then, combining with 3) and 4), the parameters of $g(SOC)$ can be derived by

$$\begin{cases} 0.3a_g + b_g = 1 \\ a_g + b_g = 1.01 \end{cases} \tag{21}$$

which yields $a_g = 5/350$, $b_g = (1 - 1.5/350)$.

In summary, the adaptive terms are designed as

$$\omega_{set} = g(SOC) = 1 + \frac{5SOC - 1.5}{350} \tag{22}$$

$$D_p = f(SOC) = \begin{cases} (4.4 - 3SOC)/350,\ p^* \geq 0 \\ (0.5 + 3SOC)/350,\ p^* < 0 \end{cases} \tag{23}$$

which can be as shown in Fig. 2. It can be seen that the relationships between SOC and the designed adaptive parameters are linear as expected.

Fig. 3 can be used to explain the process to achieve the SOC balancing. It is assumed that the system is in discharge state to supply the load and $SOC_i(t_0) - SOC_j(t_0) = \Delta SOC(t_0) > 0$ at $t = t_0$. According to (22) and (23), there are $\omega_{seti}(t_0) - \omega_{setj}(t_0) = \Delta SOC(t_0)/70 > 0$ and $D_{pi}(t_0) < D_{pj}(t_0)$. As a result, VSG$i$ will

TABLE I
SUMMARY OF EXISTING DECENTRALIZED SOC BALANCING CONTROL STRATEGIES

Existing Methods	$g(SOC)$	$dg(SOC)/dSOC$	$f(SOC)$		$df(SOC)/dSOC$	
			$p^* \geq 0$	$p^* < 0$	$p^* \geq 0$	$p^* < 0$
[10]	constant	0	$\propto 1/SOC^n,\ n>0$	not discussed	<0	not discussed
[11]	constant	0	$\propto 1/SOC^n,\ n>0$	$\propto SOC^n,\ n>0$	<0	>0
[12]	constant	0	$\propto -SOC$	not discussed	<0	not discussed
[13]	$\propto SOC$	>0	constant	not discussed	0	not discussed
Proposed method	$\propto SOC$	>0	$\propto -SOC$	$\propto SOC$	<0	>0

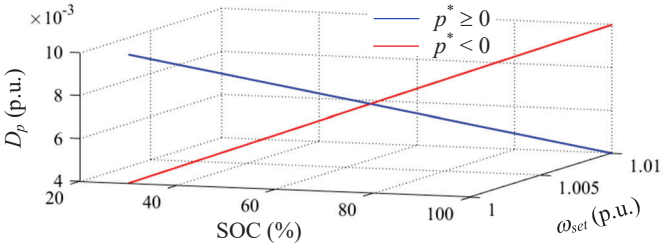

Fig. 2. Adaptive range of the parameters in proposed strategy.

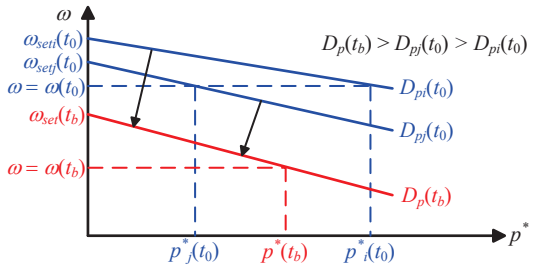

Fig. 3. Diagram of power sharing to achieve SOC balancing.

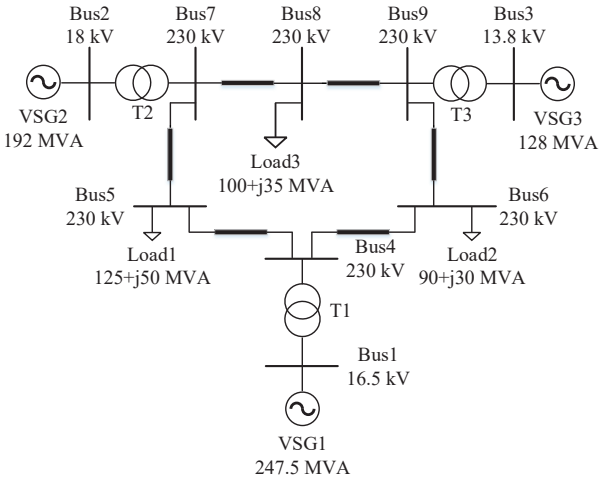

Fig. 4. Topology of IEEE 9-Bus System.

share a more active power than VSGj, i.e., $p_i^*(t_0) > p_j^*(t_0)$, and the frequency is $\omega = \omega(t_0)$. After a period of time Δt, both SOC_i and SOC_j will decrease. However, as VSGi takes a larger portion of the load, SOC_i will decrease more than SOC_j, which leads to $SOC_i(t_0+\Delta t) - SOC_j(t_0+\Delta t) = \Delta SOC(t_0+\Delta t) < \Delta SOC(t_0)$. Meanwhile, both ω_{seti} and ω_{setj} decrease while D_{pi} and D_{pj} increase to make VSGi to output less power and VSGj to more power. Nevertheless, like the condition at $t = t_0$, there still is $p_i^*(t_0+\Delta t) > p_j^*(t_0+\Delta t)$ if $\Delta SOC(t_0+\Delta t) > 0$. It is expected at some point defining as $t = t_b$ there will be $SOC_i(t_b) - SOC_j(t_b) = \Delta SOC(t_b) = 0$. At this moment, there are $\omega_{seti}(t_b) = \omega_{setj}(t_b) = \omega_{set}(t_b)$ and $D_{pi}(t_b) = D_{pj}(t_b) = D_p(t_b)$. Therefore, VSG$i$ and VSGj will share the same active power of $p^*(t_b)$. Afterwards, SOC_i will always equal to SOC_j if there is no disturbance to deviate the power sharing, and the SOC balancing is achieved. It is noticed that the frequency is decreased as well, i.e., $\omega(t_b) < \omega(t_0)$. However, the limitation of frequency has been taken into consideration when designing the controller as aforementioned, which guarantees the steady-state frequency will not break the requirements of the power system.

IV. CASE STUDIES

The IEEE 9-Bus system shown in Fig. 4 is used to demonstrate the performance of the proposed strategy, where all of the three generators are replaced by VSGs with the proposed control strategy in Fig. 1. The DC souces are Lithium-Ion batteries, where the parameters are automatically generated by the battery model in Matlab/Simulink. The initial SOCs are set to be 100%, 95%, and 90%, respectively. The other main parameters are shown in Fig. 4 and Table II. A load step with 45 MW in Load 1 is implemented at $t = 80$ s as a disturbance. Therefore, there are two factors which may lead to the SOC unbalance in the simulation, i.e., the unbalanced initial SOCs and transient power sharing during the start and load disturbance.

Fig. 5 shows the simulation results with the traditional VSG control without any SOC-balancing strategy, where $g(SOC)$ and $f(SOC)$ are constant at 1 p.u. and 0.005 p.u. It can be seen that good active power sharing can be achieved. The steady-state frequencies before and after the load disturbance are 0.9975 p.u. and 0.9972 p.u., respectively. However, it does not contribute to the SOC balancing. Table III further compares the distinctions of SOCs at different moments. At the beginning,

TABLE II
MAIN PARAMETERS OF TEST SYSTEM IN FIG. 4

Symbol	Value	Symbol	Value	Symbol	Value
H_1	9.55 s	k_{q1}	50	Q_{0_1}	0
H_2	3.33 s	k_{q2}	50	Q_{0_2}	0
H_3	5 s	k_{q3}	100	Q_{0_3}	0
D_{q1}	0.05	V_{0_1}	1.04	X_{v1}	0.24
D_{q2}	0.05	V_{0_2}	1.025	X_{v2}	1.66
D_{q3}	0.05	V_{0_3}	1.025	X_{v3}	1.61

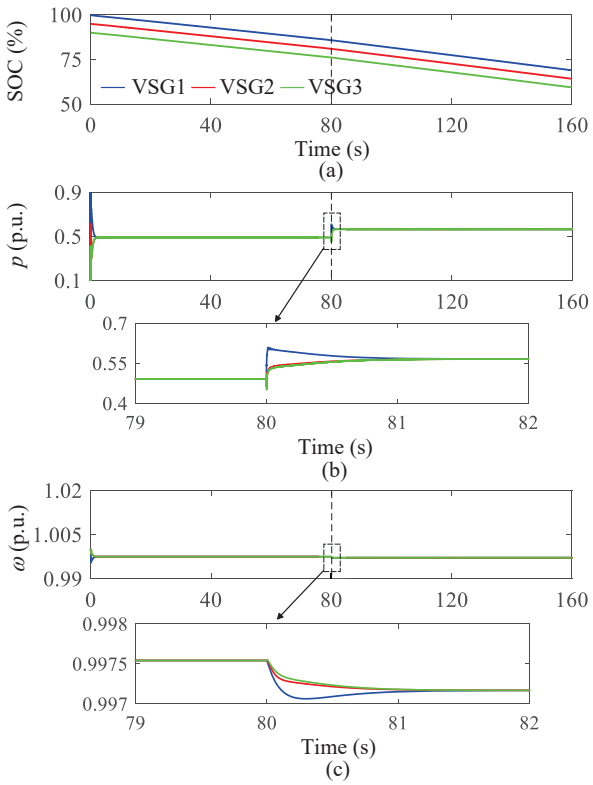

Fig. 5. Simulation results with traditional VSGs. (a) SOC. (b) Output active power. (c) Angular frequencies.

the SOC differences between VSG1 and VSG2, VSG3 are 5% and 10%, respectively. After the start process, at $t = 3$ s, they decrease to 4.8% and 9.7% due to the fact that VSG1 shares more transient power. Afterwards, these differences remain until the end of the simulation. As the load disturbance is quickly damped and does not make a large transient power unbalance, the SOC differences are not significantly influenced in this case.

As a comparison, Fig. 6 shows the simulation results with the method in [12] and the key values of SOCs are listed in Table III as well. The same specifications as in Section III-B are used to design the controller except $g(SOC)$ is constant at 1 p.u. as presented in Table I. With this method, VSG1 shares most power while VSG3 shares the least, which gradually decrease the SOC differences among VSGs. Compared with the traditional VSG, the SOC differences decrease to 4.7% and

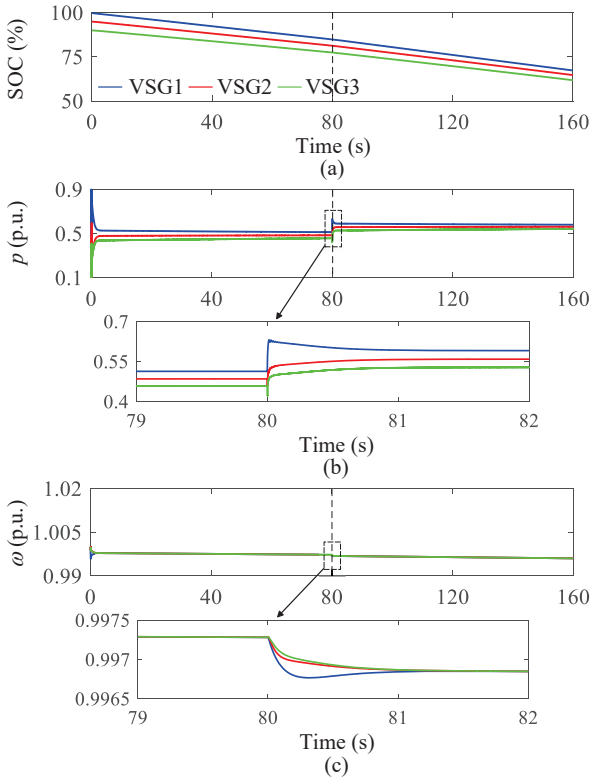

Fig. 6. Simulation results with control method in [12]. (a) SOC. (b) Output active power. (c) Angular frequency

9.6% after the start. Afterwards, these values can be further decreased. At the end of the simulation, they are as small as 2.6% and 5.5%, which are 54.2% and 56.7% of those with the traditional VSG, respectively. However, there still are obvious SOC unbalance, which is due to the limitations of $f(SOC)$. Meanwhile, the change of $f(SOC)$ leads the frequencies to be slightly smaller than those in Fig. 5, which are 0.9961 p.u. at the end.

Fig. 7 presents the simulation results with the proposed controlmethod. As shown, VSG1 shares much more power than VSG3. Compared with Fig. 6(a), the proposed method has faster response to balance the SOCs. From Table I, the differences of SOCs are much smaller than those with the traditional VSG and the method in [12]. In the end of the simulation, the values of $SOC_1 - SOC_2$ and $SOC_1 - SOC_3$ are only 0.3% and 0.8%, where they are only 11.5% and 14.5% of those with the method in [12]. As the SOCs are balanced, the output powers gradually equal as well. The angular frequencies are also shown in Fig. 7, which are well limited in the specifications (0.99-1.02 p.u. as in Section III-B) and they are higher than those in Fig. 5 and Fig. 6. In the end of the simulation, the frequencies are 1.001 p.u., which is because the adaptive $g(SOC)$ is larger than 1 p.u. in the specified range of SOC to lift the frequency. Meanwhile, by comparing the waveforms of the power and frequency, it implies that the proposed method will hardly influence the dynamics of the power control loop responding to a load disturbance. This is

TABLE III
COMPARISONS OF DISTINCTIONS OF SOCS AT DIFFERENT INSTANTS OF THE THREE METHODS

Methods	$SOC_1 - SOC_2$ (%)					$SOC_1 - SOC_3$ (%)				
	$t = 0$ s	$t = 3$ s	$t = 79$ s	$t = 82$ s	$t = 160$ s	$t = 0$ s	$t = 3$ s	$t = 79$ s	$t = 82$ s	$t = 160$ s
Traditional VSG	5	4.8	4.8	4.8	4.8	10	9.7	9.7	9.7	9.7
Ref. [12]	5	4.7	3.6	3.5	2.6	10	9.6	7.4	7.4	5.5
Proposed method	5	4.6	1.3	1.2	0.3	10	9.4	3	2.9	0.8

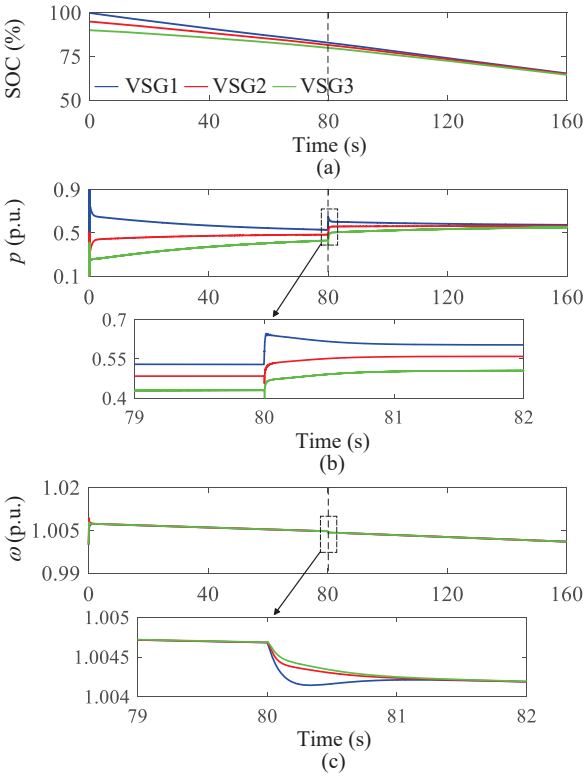

Fig. 7. Simulation results with proposed control method. (a) SOC. (b) Output active power. (c) Angular frequency.

because the variation of SOC has a much slower dynamics. Actually, small capacities are used in the simulation in order to decrease the simulation time. In practice, much larger capacities may be used to guarantee a long-term supply, which implies a slower SOC dynamics. Therefore, some favorable features of the VSG such as the inertia characteristics are not significantly changed.

V. CONCLUSION

In this paper, a completely decentralized adaptive control strategy for VSG-based islanded power grid is proposed to realize the SOC balancing. The general requirements of the adaptive terms are given in both charging and discharging states. Furthermore, the simple linear relationships are used to construct a new controller. By adaptively changing the parameters of the virtual governor based on the local SOC, multiple specifications such as stability and steady-state frequency can be achieved without any communication network. Meanwhile, the simulation results show that the proposed method ensures a fast response of the SOC balancing and can keep the favorable features of the VSG.

REFERENCES

[1] M. Chen, D. Zhou, and F. Blaabjerg, "Modelling, implementation, and assessment of virtual synchronous generator in power systems," *J. Mod. Power Syst. Clean Energy*, vol. 8, no. 3, pp. 399–411, May 2020.

[2] A. Fernández-Guillamón, E. Gómez-Lázaro, E. Muljadi, and Á. Molina-García, "Power systems with high renewable energy sources: A review of inertia and frequency control strategies over time," *Renew. Sustain. Energy Rev.*, vol. 115, pp. 1–12, Nov. 2019.

[3] M. Chen, D. Zhou, and F. Blaabjerg, "Characteristics of virtual synchronous generator based voltage source converter," in *2020 IEEE Power Energy Soc. Gen. Meet.*, pp. 1–5.

[4] X. Quan, R. Yu, X. Zhao, Y. Lei, T. Chen, C. Li, and A. Q. Huang, "Photovoltaic synchronous generator: Architecture and control strategy for a grid-forming PV energy system," *IEEE J. Emerg. Sel. Top. Power Electron.*, vol. 8, no. 2, pp. 936–948, Jun. 2020.

[5] C. Sun, G. Joos, and F. Bouffard, "Adaptive coordination for power and SoC limiting control of energy storage in an islanded AC microgrid with impact load," *IEEE Trans. Power Deliv.*, no. 2, pp. 580–591, Apr.

[6] M. Chen, D. Zhou, and F. Blaabjerg, "Active power oscillation damping based on acceleration control in paralleled virtual synchronous generators system," *IEEE Trans. Power Electron.*, vol. 36, no. 8, pp. 9501–9510, Aug. 2021.

[7] N. L. Díaz, A. C. Luna, J. C. Vasquez, and J. M. Guerrero, "Centralized control architecture for coordination of distributed renewable generation and energy storage in islanded AC microgrids," *IEEE Trans. Power Electron.*, vol. 32, no. 7, pp. 5202–5213, Jul. 2017.

[8] D. Li, Z. Wu, B. Zhao, and L. Zhang, "An improved droop control for balancing state of charge of battery energy storage systems in AC microgrid," *IEEE Access*, vol. 8, pp. 71 917–71 929, 2020.

[9] T. Wu, Y. Xia, L. Wang, and W. Wei, "Multiagent based distributed control with time-oriented SoC balancing method for dc microgrid," *Energies*, vol. 13, no. 11, pp. 1–17, Jun. 2020.

[10] X. Lu, K. Sun, J. M. Guerrero, J. C. Vasquez, and L. Huang, "State-of-charge balance using adaptive droop control for distributed energy storage systems in DC microgrid applications," *IEEE Trans. Ind. Electron.*, vol. 61, no. 6, pp. 2804–2815, Jun. 2014.

[11] X. Lu, K. Sun, J. M. Guerrero, J. C. Vasquez, and L. Huang, "Double-quadrant state-of-charge-based droop control method for distributed energy storage systems in autonomous DC microgrids," *IEEE Trans. Smart Grid*, vol. 6, no. 1, pp. 147–157, Jan. 2015.

[12] Q. Wu, R. Guan, X. Sun, Y. Wang, and X. Li, "SoC balancing strategy for multiple energy storage units with different capacities in islanded microgrids based on droop control," *IEEE J. Emerg. Sel. Top. Power Electron.*, vol. 6, no. 4, pp. 1932–1941, Dec. 2018.

[13] X. Sun, Y. Hao, Q. Wu, X. Guo, and B. Wang, "A multifunctional and wireless droop control for distributed energy storage units in islanded AC microgrid applications," *IEEE Trans. Power Electron.*, vol. 32, no. 1, pp. 736–751, Jan. 2017.

[14] X. Lin, R. Zamora, and C. A. Baguley, "A fully filter-based decentralized control with state of charge balancing strategy for battery energy storage systems in autonomous DC microgrid applications," *IEEE Access*, vol. 9, pp. 15 028–15 040, 2021.

[15] D. Xu, A. Xu, C. Yang, and P. Shi, "Uniform state-of-charge control strategy for plug-and-play electric vehicle in super-ups," *IEEE Trans. Transp. Electrif.*, vol. 5, no. 4, pp. 1145–1154, 2019.